A retractable electron emitter for the creation of unperturbed pure electron plasmas

John W. Berkery,[a] Thomas Sunn Pedersen, and Luis Sampedro
Department of Applied Physics and Applied Mathematics, Columbia University, New York, New York 10027

(Received 14 September 2006; accepted 28 November 2006; published online 30 January 2007)

A retractable electron emitter has been constructed for the creation of unperturbed pure electron plasmas on magnetic surfaces in the Columbia Non-neutral Torus stellarator. The previous method of electron emission using emitters mounted on stationary rods limited the confinement time to 20 ms. A pneumatically driven system that can retract from the magnetic axis to the last closed flux surface in less than 20 ms while filling the surfaces with electrons was designed. The motion of the retractable emitter was modeled with a system of dynamical equations. The measured position versus time of the emitter agrees well with the model and the fastest axis-to-edge retraction was measured to be 20 ms with 40 psig helium gas driving the pneumatic piston. © *2007 American Institute of Physics.* [DOI: 10.1063/1.2431090]

I. INTRODUCTION

In recent years the desire for increased confinement time in stellarators has led to very complex magnetic field coils. Stellarators with simpler coil sets tend to suffer from poor confinement, except when large electric fields are present. Radial electric fields can enhance stellarator confinement by reducing neoclassical and turbulent transport.[1] In a quasi-neutral plasma, one is generally limited to using either modest self-generated ambipolar electric fields, or external fields driven with biased probes.[2] Even greater improvements in confinement time are predicted for large electric fields $q\Phi/T \gg 1$. This regime can be explored experimentally in a non-neutral plasma. The Columbia Non-neutral Torus[3] studies the regime of very high electric fields in stellarators and their effect on the confinement time.

It is necessary to create a pure electron plasma that is unperturbed in order to determine the confinement time. Presently the plasmas are created with stationary electron emitters, but the presence of the emitter rods in the plasma drives a loss of electrons and limits the observed confinement time to 20 ms.[4] Alternatively, the electron plasmas could be created by injection from outside the magnetic surfaces, as has been employed in the Compact Helical System (CHS),[5] or by using a retractable electron emitter that creates the plasma while moving through, and ultimately leaving, the magnetic surfaces. We have chosen the latter method because of its potential efficiency for filling the surfaces with electrons. To the authors' knowledge this is the first attempt to create a pure electron plasma with a retractable electron emitter system. This system might also be useful for creating pure electron plasmas in purely toroidal magnetic geometries, where methods of efficient injection of electrons have encountered considerable difficulties.[6–11]

The goal of this work is to create a retractable electron emitter that can produce a pure electron plasma in the Columbia Non-neutral Torus (CNT) while dwelling in the plasma for less than 20 ms. To accomplish this we have designed a pneumatic actuation system and modeled the retraction of the emitter with a nonlinear model of the pneumatic system. The retractable emitter system was then tested in the CNT facility utilizing helium as the working gas. These plasmas will subsequently be diagnosed by capacitive copper sector probes, so that the plasmas will be created and diagnosed in a purely unperturbed manner. This will enable the ultimate goal of studying the possible confinement improvements in a non-neutral stellarator plasma due to high electric fields.

In Sec. II the design of the retractable electron emitter system, including the design requirements and the detailed layout of the structure, is presented. In Sec. III, a nonlinear model of the motion of the emitter is developed. This includes the equations of motion, pressurization of the cylinder, and mass flow through the solenoid valve. Section IV details the performance of the emitter and comparisons of the measurements and the modeled behavior. Finally, the conclusions of this work are drawn.

II. DESIGN

The main requirements of the design of the retractable electron emitter are that the emitter is able to adequately fill the magnetic surfaces with a pure electron plasma of the order of about 10^{12} m^{-3} density while moving from the magnetic axis to the edge in less than 20 ms. To retract the emitter as quickly as possible it is advantageous to intersect the plasma at its smallest thickness (a minor radius of about 6.7 cm), which in the CNT geometry means coming through a flange on the top of the vacuum vessel (at 21° from vertical, see Fig. 1). Thus the entire system must be rigidly supported by the ceiling. In order to efficiently fill the magnetic surfaces with a pure electron plasma, the emitter bias must be changed as a function of position during the retraction so that the potential profile of the created plasma is close to the

[a]Electronic mail: jwb2112@columbia.edu

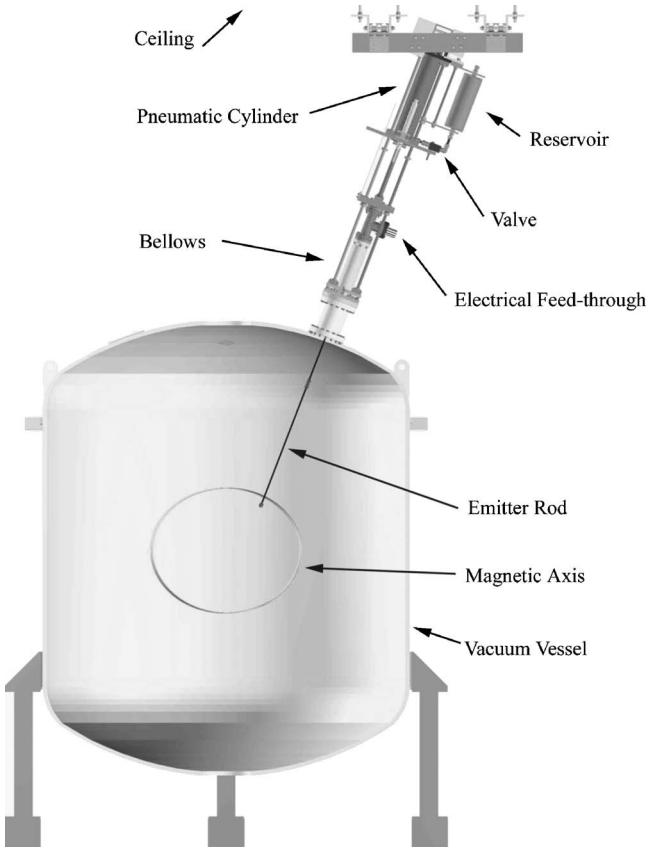

FIG. 1. Full view of the retracting electron emitter system, including a cut-away view of the vacuum tank, and a representation of the magnetic axis.

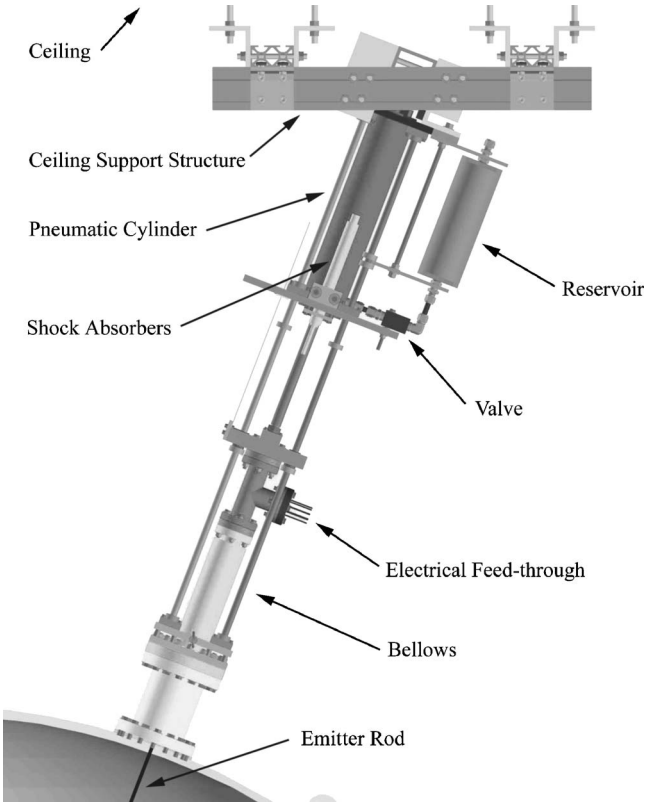

FIG. 2. Detailed view of the retracting electron emitter system.

equilibrium potential profile. A circuit to accomplish this is currently being built. Finally, another requirement is that the emitter rods and the filaments must be able to handle the resulting acceleration and deceleration of the retraction.

Similar systems have been previously used to diagnose fusion plasmas. Some examples include the reciprocating pneumatic probes that were used in the DIII-D,[12] Alcator C-Mod,[13] and TEXTOR[14] tokamaks, while in the ASDEX[15] tokamak, the reciprocating Langmuir probe was electrically actuated. A reciprocating pneumatic Langmuir probe system was also used on the TJ-II stellarator.[16] All of these systems required the probe to quickly reciprocate in and out of the plasma. On CNT the retracting emitter system is used to create the plasma and therefore the emitter may be held stationary in the magnetic field region before the plasma is created and must merely move in one direction (outward). This simplifies the design somewhat.

The retracting electron emitter design consists of the following system (see Fig. 2). A pneumatic cylinder (Clippard UDR-48–10) is used to actuate the emitter rod. The emitter is initially positioned on the far side of the magnetic axis so that most of the acceleration takes place prior to passing through the axis. The maximum velocity is in the region from the axis to the edge, where the plasma is created, thus minimizing the dwell time of the emitter. The emitter itself is a tungsten coil from a halogen light bulb. It is mounted in a small Macor piece attached to a quarter inch diameter stainless steel tube. The coil and Macor assembly was tested for its ability to withstand the acceleration and deceleration forces before the system was mounted to the vacuum chamber. The stainless steel tube is insulated with alumina for about 20 in. of length (greater than the length that will be in the plasma region). This emitter rod is welded to a doubled-sided conflat flange on the far side of a vacuum bellows. On the near side (tank side) of the bellows, the emitter rod is supported by another doubled-sided conflat flange with a clearance hole (see Fig. 3). The emitter power is fed through a UHV electrical feed-through mounted on a tee on the far side of the bellows. The tee is then connected to a blank conflat flange and an aluminum plate that in turn is connected to the pneumatic cylinder rod. On this plate are mounted four linear ball bearings which run smoothly on half inch stainless steel shafts. When the plate is fully retracted it runs into two shock absorbers which decelerate the moving assembly over its last two inches of travel.

The pneumatic cylinder derives its power from a pressurized reservoir of gas that is connected to the cylinder through a solenoid valve (Parker B6V2BB553A). When the valve is opened, the cylinder chamber is pressurized and the piston moves, retracting the moving assembly and emitter rod. A mathematical model of this process is presented in the next section.

The position versus time of the emitter is measured with a simple optical system. It consists of a perforated strip (10 holes per inch) that is attached to the moving assembly and moves through a photomicrosensor. The photomicrosensor is a device with a small light-emitting diode (LED) that illuminates a phototransistor so that when the path is blocked a voltage is output but when the path is free the voltage drops

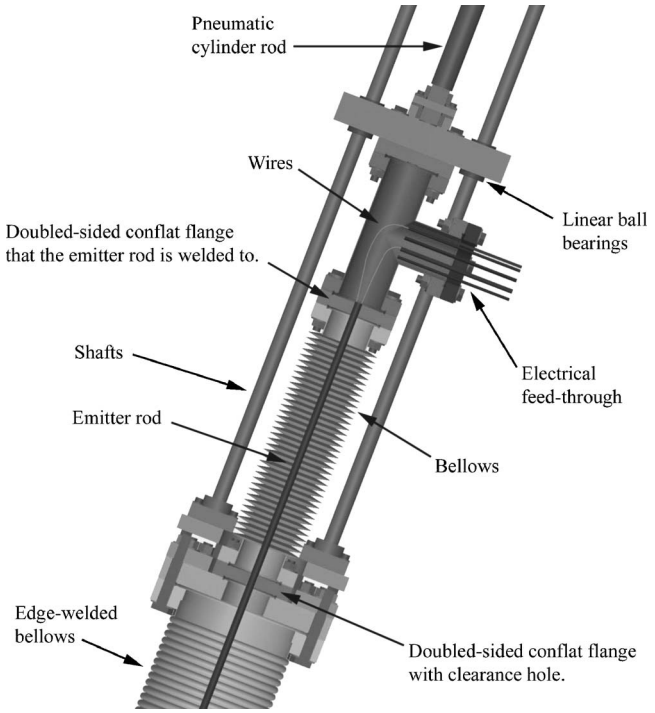

FIG. 3. Cut-away view of the bellows and emitter rod system.

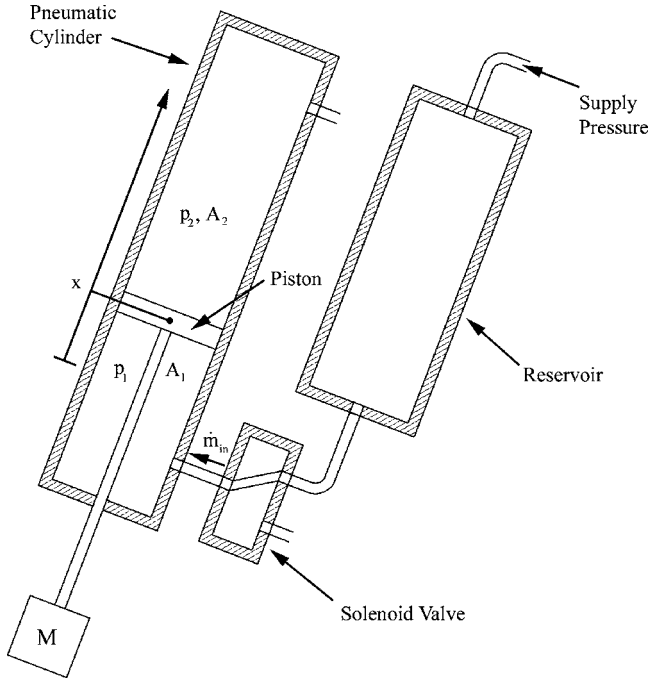

FIG. 4. Schematic of the pneumatic system.

to zero. Thus, the perforated strip moving through the path of the photomicrosensor alternatively shows zero or about three volts every tenth of an inch, and the signal can be interpreted to measure position versus time.

Finally, the entire structure is mounted to the ceiling of the laboratory with a ceiling support structure that allows for slight adjustment in each dimension and one tilt angle so that the emitter can be positioned to perfectly intersect the magnetic axis. Once the desired position is achieved (by means of magnetic field mapping, as in Ref. 17) the structure is tightened down and secured. The small movements are accommodated at the rigid vacuum tank flange by a moderately flexible formed bellows. The complete system is shown in Fig. 1.

III. MODEL OF THE EMITTER RETRACTION

In order to determine whether the designed system would meet the requirements, especially the requirement of retraction through the plasma region in less than 20 ms, a model of the retraction was sought. The dynamics of a pneumatic system is a problem that has been previously considered.[18,19] We will follow the treatment of Richer and Hurmuzlu,[20] as it concerns a system similar to ours. The nonlinear system of equations begins with an equation of motion

$$M\ddot{x} = p_1A_1 - p_2A_2 - Mg\cos\theta - p_{\text{atm}}A_b - k_b(x - x_n). \quad (1)$$

Here, M is the mass that is being moved in the direction of x (including the piston and rod masses) and x increases from 0 at the starting position. The driving force is p_1A_1, the pressure times the area on the inlet side of the cylinder (see Fig. 4). This force is opposed by the pressure times the area in the outlet side of the cylinder, p_2A_2, the gravitational force (here acting at an angle θ=21°), the atmospheric pressure pushing on the evacuated bellows (with effective cross-sectional area A_b), and the spring force of the bellows (where k_b is the spring constant and x_n is the neutral position of the spring). We have neglected both static and viscous friction.

Assuming the evacuation of the outlet side of the cylinder occurs with minimal pressure differential to atmospheric pressure, $p_2=p_{\text{atm}}$ throughout the retraction. Then Eq. (1) represents an equation for $x(t)$ that is dependent only on $p_1(t)$. The equation for the pressurization of a pneumatic cylinder chamber has been shown to be[20]

$$\dot{p}_1 = \frac{RT}{V_{10} + A_1x}(\alpha_{\text{in}}\dot{m}_{\text{in}}) - \frac{p_1A_1}{V_{10} + A_1x}(\alpha\dot{x}). \quad (2)$$

In this equation R is the ideal gas constant, T is the gas temperature, V_{10} is the initial volume of chamber 1 (the inlet side of the cylinder), $\dot{m}_{\text{in}}$ is the mass flow rate of gas into chamber 1, and α and α_{in} are coefficients between 1, for an isothermal process, and k (the specific heat ratio), for an adiabatic process. The working gas was helium. This equation shows that the pressure increases due to mass flow into the chamber, but is reduced by the expanding volume of the chamber as the piston moves. It is assumed that there is no leakage of the piston seal.

We now have two nonlinearly coupled equations for p_1 and x and are left with the unknown $\dot{m}_{\text{in}}$. Because of the short lengths of the connecting tubes between the reservoir and valve and between the valve and cylinder, we will consider the effect of these tubes to be negligible and model the mass flow rate into the cylinder strictly as the flow across the valve orifice. If the valve has an orifice area of $A_v(t)$ which increases in time until the valve is fully open, and the reservoir pressure is p_0, then the mass flow rate is given by

TABLE I. Table of constants specified by the design that are used in the model.

M (kg)	A_1 (m)	A_2 (m)	θ (deg)
6.4	4.2×10^{-3}	4.5×10^{-3}	21
A_b (m)	k_b (kg/s^2)	x_n (m)	V_{10} (m^3)
1.8×10^{-3}	216	0.45	$\approx4\times10^{-5}$

$$\dot{m}_{\text{in}} = \begin{cases} C_f A_v \dfrac{p_0}{\sqrt{T}} C1 \text{ if } \dfrac{p_1}{p_0} \le p_{\text{cr}} \\ C_f A_v \dfrac{p_0}{\sqrt{T}} C_2 \left(\dfrac{p_1}{p_0}\right)^{1/k} \sqrt{1-\left(\dfrac{p_1}{p_0}\right)^{(k-1)/k}} \text{ if } \dfrac{p_1}{p_0} > p_{\text{cr}}. \end{cases} \tag{3}$$

When the pressure ratio across the orifice is smaller than the critical pressure ratio p_{cr}, the flow is choked and the first expression applies. When the pressure ratio is larger than p_{cr}, the second expression applies. In these expressions, C_f is the valve discharge coefficient, a constant that will be discussed in greater detail later. The critical pressure ratio and the constants C_1 and C_2 are given by

$$p_{\text{cr}} = \left(\frac{2}{k+1}\right)^{k/(k-1)}, \tag{4}$$

$$C_1 = \sqrt{\frac{k}{R}\left(\frac{2}{k+1}\right)^{(k+1)/(k-1)}}, \tag{5}$$

$$C_2 = \sqrt{\frac{k}{R}\left(\frac{2}{k-1}\right)}. \tag{6}$$

Because p_0 is constant in the reservoir, Eq. (3) specifies $\dot{m}_{\text{in}}$ as a function of p_1 and thus closes the system of equations for x, p_1, and $\dot{m}_{\text{in}}$. What is left to be specified are the various constants in the equations and the area of the valve A_v as a function of time as it opens. If we make the simplifying assumption that the spool of the solenoid valve moves with a constant velocity, exposing the circular valve orifice in a time τ_v, it can be shown that the orifice area as a function of time is[20]

$$A_v = 2R_v^2\left[\arctan\left(\sqrt{\frac{t}{\tau_v - t}}\right) - \left(1-\frac{2t}{\tau_v}\right)\sqrt{\frac{t}{\tau_v}-\left(\frac{t}{\tau_v}\right)^2}\right], \tag{7}$$

from $t=0$ to $t=\tau_v$, after which $A_v=\pi R_v^2$.

The parameters M, A_1, A_2, θ, A_b, k_b, x_n, and V_{10} are constants of the design and are specified in Table I. Note that the value of V_{10} is estimated, but the model is very insensitive to this parameter. The ratio of specific heats k is 1.66 and the ideal gas constant R, is 2.077×10^3 for helium. The temperature T is taken to be room temperature and the reservoir pressure p_0 is varied. Following Richer and Hurmuzlu,[20] we will estimate $\alpha=1.2$ and $\alpha_{\text{in}}=k$. For the Parker solenoid valve, the orifice radius $R_v=3.175\times10^{-3}$ m, and the valve opening time $\tau_v=0.037$ s.

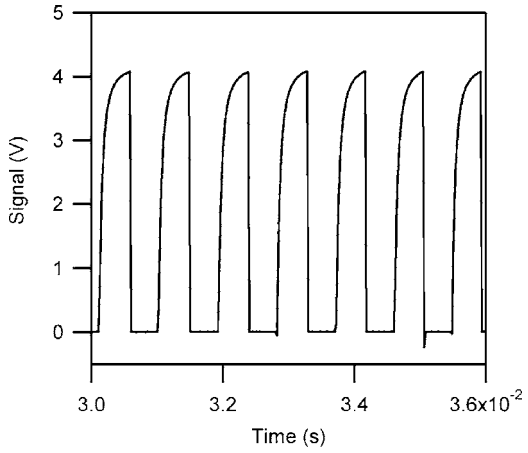

FIG. 5. Voltage on the photomicrosensor vs time. Each positive-slope crossing of 2 V represents a movement of 0.1 in.

The remaining free parameter is the valve flow coefficient C_f. Previous to the construction of the retractable electron emitter system, the valve flow coefficient was not known. A range of values of C_f was tested in the model which gave a reasonable range of results for the expected retraction time, so the construction of the device was commenced. Subsequently, a constant value of $C_f=0.4$ was found to give good agreement between the model and the measurements of position versus time for the pressure range of 25–40 psig, as shown in the next section. Although it is possible to independently measure the value of C_f by directly measuring the mass flow rate out of the valve at given pressure ratios and comparing to Eq. (3),[20] it was determined that this step was not necessary for our purposes. The comparisons of the model to measurements presented in the next section use the empirically determined value of $C_f=0.4$ to give the best agreement between the model and measurements.

Equations (1)–(3) and (7) were solved for $x(t)$ in Matlab using an ordinary differential equation solver and all the input parameters listed above. When the moving assembly reaches the shock absorbers, a force is added to the right-hand side of Eq. (1) that slows the motion to zero velocity. The two shock absorbers act as spring dampers and the force takes the form

$$F_s = 2(-k_s x - c_s e^{x/l}\dot{x}), \tag{8}$$

where $k_s=350$ kg/s^2 is the spring constant and $c_s=50$ kg/s is the initial viscous damping coefficient. The viscous damping of the shock absorbers can be approximated to increase exponentially over a length scale $l=0.033$ m. Each of these coefficients was empirically determined.

The solutions of the model for $x(t)$ were found to be relatively insensitive to small estimation errors or changes in the input parameters listed above except for the valve flow coefficient and of course the reservoir pressure, which is a user controlled variable.

IV. PERFORMANCE OF THE RETRACTABLE EMITTER

The position of the emitter versus time was measured (in a relative sense) by the photomicrosensor system previously described (see Sec. II). A typical output of the sensor is

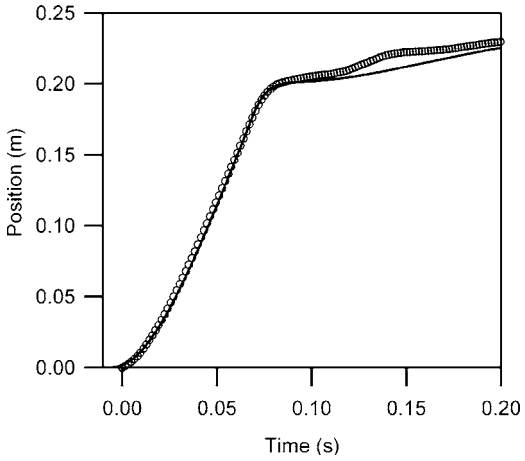

FIG. 6. Position vs time measurement and model for helium gas at 40 psig. The markers are the measured points and the line is the modeled velocity.

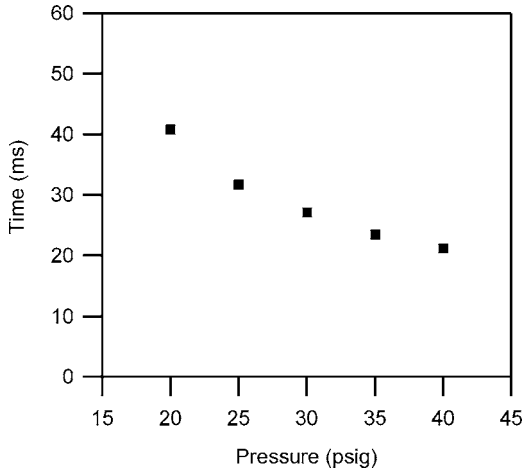

FIG. 8. The time that the emitter tip spends between the magnetic axis and the last closed flux surface vs pressure.

shown in Fig. 5. Each period of the square wave indicates that the emitter has moved 0.1 in. This data is then plotted as position versus time, and differentiated to find the velocity as well. Figure 6 shows the position versus time data for the case of $p_1=40$ psig. This data is compared to the predicted position from the model described in Sec. III. The model fits the data quite well because of the selection of the proper value for the parameter C_f.

Figure 7 shows the velocity of the emitter versus time. The velocity quickly increases to a relatively constant value of about 3.2 m/s in this case, before the moving assembly meets the shock absorbers. Once the shock absorbers are engaged, the velocity drops off quickly as the assembly is stopped. The model predicted velocity versus time is also shown in this figure.

Originally the design of the retracting electron emitter did not include a reservoir, i.e., the helium tank was connected directly to the valve inlet with ten foot long tubing. It was found, however, that in this case the velocity of the emitter began to *decrease* before the shock absorbers were reached. This was due to the long tube connecting the pressure supply to the valve, so that when the velocity of the piston became too great the pressure dropped [due to the expanding volume, as seen by the second term of Eq. (2)] and the remote pressure supply was unable to quickly compensate for this pressure drop, hence the velocity dropped as well. The reservoir was subsequently added to address this issue. The overshoot of the modeled velocity in Fig. 7 could be due to the constant pressure assumption in the model. In reality, because the reservoir is still of finite size, the piston inlet pressure will drop slightly as the piston retracts.

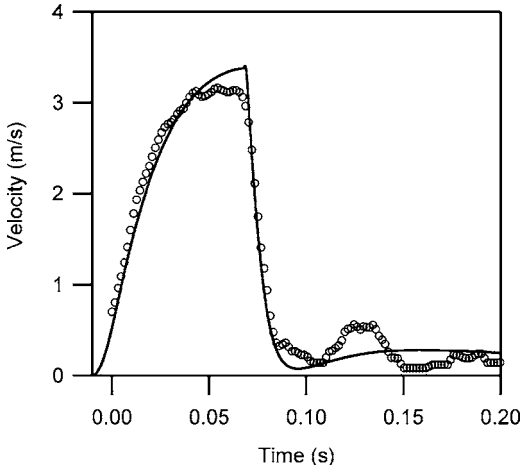

FIG. 7. Velocity vs time measurement and model for helium gas at 40 psig. The markers are the measured points and the line is the modeled velocity.

At the end of the motion, the shock absorbers are seen to go through two phases, a quick deceleration followed by a relatively slow and uneven compression of the shock absorber for the rest of the stroke. Shock absorbers that decelerate the load more smoothly over the whole stroke would be preferable, but the current system sufficiently provides a deceleration force that is comparable to, although greater than, the acceleration force when the system begins moving. The acceleration force reaches about 12 g for the fastest operation, and the deceleration force can be as high as 23 g. Over many repeated tests, this level of acceleration has not damaged the emitter filament or any other component of the system.

By knowing the starting position of the emitter on the far side of the magnetic axis, the time the emitter spends in the plasma can be determined from the position versus time data. This is calculated by simply subtracting the time at which the emitter reaches the axis from the time when it reaches the last closed flux surface. Figure 8 shows the axis-to-edge retraction time versus the pressure used. At a pressure of $p_1=40$ psig, the system meets the goal of 20 ms. Because the deceleration force is very high, it was decided that pushing the retraction to higher velocities in order to gain a small decrease in the retraction time to below 20 ms was not worth the risk of breaking the device.

V. CONCLUSIONS

A retractable electron emitter for the Columbia Nonneutral Torus has been designed, constructed, and tested. The motivation for creating such a system was that the previously employed stationary emitter rods drove transport of electrons and therefore limited the confinement to 20 ms. A model of

the emitter motion showed that a fast retraction from the magnetic axis to the last closed flux surface was possible. Measurements of the position versus time matched well with the model. The fastest measured retraction, using 40 psig of helium to drive the pneumatic piston, was 20 ms.

ACKNOWLEDGMENTS

The authors would like to thank Andrei Petrenko for his help constructing and installing the retractable emitter system. This work is supported by the Fusion Energy Sciences Postdoctoral Research Program of the U.S. Department of Energy.

[1] M. Kick, H. Maassberg, M. Anton, J. Baldzuhn, M. Endler, C. Gomer, M. Hirsch, A. Weller, and S. Zoletnik, Plasma Phys. Controlled Fusion **41**, A549 (1999).
[2] C. Hidalgo, M. A. Pedrosa, N. Dreval, K. J. McCarthy, L. Eliseev, M. A. Ochando, T. Estrada, I. Pastor, E. Ascasíbar, E. Calderón, A. Cappa, A. A. Chmyga, A. Fernández, B. Gonçalves, J. Herranz, J. A. Jiménez, S. M. Khrebtov, A. D. Komarov, A. S. Kozachok, L. Krupnik, A. López-Fraguas, A. López-Sánchez, A. V. Melnikov, F. Medina, B. van Milligen, C. Silva, F. Tabarés, and D. Tafalla, Plasma Phys. Controlled Fusion **46**, 287 (2004).
[3] T. S. Pedersen, A. Boozer, J. Kremer, R. Lefrancois, W. Reiersen, F. Dahlgreen, and N. Pomphrey, Fusion Sci. Technol. **46**, 200 (2004).
[4] J. Kremer, T. S. Pedersen, Q. Marksteiner, and R. Lefrancois, Phys. Rev. Lett. **97**, 095003 (2006).
[5] H. Himura, H. Wakabayashi, M. Fukao, M. Isobe, S. Okamura, and H. Yamada, IEEE Trans. Plasma Sci. **32**, 510 (2004).
[6] M. Stoneking, P. Fontana, R. Sampson, and D. Thuecks, Phys. Plasmas **9**, 766 (2002).
[7] J. Daugherty, J. Eninger, and G. Janes, Phys. Fluids **12**, 2677 (1969).
[8] W. Clark, P. Korn, A. Mondelli, and N. Rostoker, Phys. Rev. Lett. **37**, 592 (1976).
[9] P. Zaveri, P. John, K. Avinash, and P. Kaw, Phys. Rev. Lett. **68**, 3295 (1992).
[10] S. Khirwadkar, P. John, K. Avinash, A. Agarwal, and P. Kaw, Phys. Rev. Lett. **71**, 4334 (1993).
[11] C. Nakashima, Z. Yoshida, H. Himura, M. Fukao, J. Morikawa, and H. Saitoh, Phys. Rev. E **65**, 036409 (2002).
[12] J. Watkins, J. Salmonson, R. Moyer, R. Doerner, R. Lehmer, L. Schmitz, and D. N. Hill, Rev. Sci. Instrum. **63**, 4728 (1992).
[13] B. LaBombard, S. Gangadhara, B. Lipschultz, S. Lisgo, D. A. Pappas, C. S. Pitcher, P. Stangeby, and J. Terry, J. Nucl. Mater. **266–269**, 571 (1999).
[14] J. Boedo, D. Gray, L. Chowal, R. Conn, B. Hiller, and K. H. Finken, Rev. Sci. Instrum. **69**, 2663 (1998).
[15] N. Tsois, C. Dorn, G. Kyriakakis, M. Markoulaki, M. Pflug, G. Schramm, P. Theodoropoulos, P. Xantopoulos, M. Weinlich, and the ASDEX Upgrade Team, J. Nucl. Mater. **266–269**, 1230 (1999).
[16] M. Pedrosa, A. López-Sánchez, C. Hidalgo, A. Montoro, A. Gabriel, J. Encabo, J. de la Gama, L. M. Martínex, E. Sánchez, R. Pérez, and C. Sierra, Rev. Sci. Instrum. **70**, 415 (1999).
[17] T. S. Pedersen, J. Kremer, R. Lefrancois, Q. Marksteiner, X. Sarasola, and N. Ahmad, Phys. Plasmas **13**, 012502 (2006).
[18] J. Shearer, Trans. ASME **78**, 233 (1956).
[19] J. Shearer, Trans. ASME **78**, 243 (1956).
[20] E. Richer and Y. Hurmuzlu, J. Dyn. Syst., Meas., Control **122**, 416 (2000).